Interactions of Cadmium-106 with Alpha Particles*

RICHARD L. HAHN†
Chemistry Department, Brookhaven National Laboratory, Upton, New York
(Received 2 November 1964)

The excitation functions of the (α,γ), (α,n), (α,p), $(\alpha,2n)$, (α,pn), $(\alpha,3n)+(\alpha,p2n)$, $(\alpha,\alpha n)$, and $(\alpha,2\alpha n)$ reactions of Cd^{106} have been determined with alpha particles of 6–39-MeV kinetic energy. Reactions involving charged-particle emission compete quite favorably with those involving neutron emission only; the large Coulomb barrier for charged-particle emission is partially offset by the relatively low separation energies for these charged particles, as compared to those for neutrons. Thus, some of the peak cross sections (and corresponding alpha-particle energies) are: (α,n), 626 mb (19 MeV); (α,p), 243 mb (22 MeV); $(\alpha,2n)$, 427 mb (32 MeV); (α,pn), 230 mb (35 MeV); and $(\alpha,\alpha n)$, 205 mb (37 MeV). Comparison of these data with the previously determined excitation functions for Sn^{124} clearly demonstrates that the reactions leading to charged-particle emission in neutron-deficient Cd^{106} are much more probable than are the analogous reactions on neutron-excess Sn^{124}. The ratio of the sum of cross sections involving the emission of at least one charged particle to the sum of cross sections for the emission only of neutrons is more than an order of magnitude greater for Cd^{106} than for Sn^{124}. This behavior may be reproduced with the statistical theory of nuclear reactions, by using $r_o=1.7$ F for the radius parameter and $a=1.8$/MeV for the level-density parameter. Detailed comparison of the data with compound nucleus theory shows good agreement for the (α,n), (α,p), and $(\alpha,\alpha n)$ excitation functions. A brief discussion of the principles of 4π scintillation counting is also presented.

I. INTRODUCTION

RECENT studies of the interactions of alpha particles with[1] Sn^{124} and[2] Ag^{107} have demonstrated that reactions in which charged particles are emitted account for an appreciable fraction of the total reaction cross section although the Coulomb barrier (for protons) is of the order of 8 MeV. The competition between neutron and proton emission should be a function of the Coulomb barrier and of the difference in separation energies of these particles in the excited nucleus. For a given nucleus, it can be shown[3] that the difference in separation energies for neutron and proton is dependent upon $(N-Z)$, the difference in the number of neutrons and protons in the nucleus. Thus, a study of nuclear reactions in nuclei of similar atomic number, but with quite different relative numbers of neutrons and protons, should accentuate the effects that differences in particle-separation energies have upon these reactions.

In this paper, then, the reactions of alpha particles with $_{48}Cd^{106}$ will be discussed and compared with similar data for $_{50}Sn^{124}$. Comparison of the data with the predictions of the compound nucleus model of nuclear reactions will be made in order to determine if the excitation functions do indeed depend on particle separation energies in the manner described by the model. Also, all of the products formed from the reactions of Cd^{106} and alphas of $\leqslant 40$ MeV are radioactive, with the exception of Cd^{108}, and of course, Cd^{106}. Hence, one can obtain a measure of the total reaction cross section over an extended energy interval and compare this with cross section values calculated with the aid of continuum theory[3,4] or the optical model.[5]

II. EXPERIMENTAL PROCEDURES

A. Targets

The targets were prepared by electroplating enriched Cd^{106} from an alkaline cyanide solution onto 0.00025-in. gold foil. The gold foils were weighed on a microanalytical balance before and after the plating procedure to determine the weight of the cadmium plate. Spectrophotometric determinations of the amount of cadmium on weighed gold foils agreed to within 5% with the values obtained from the weighings; these spectrochemical procedures also demonstrated that the cadmium deposits were uniform in thickness to within 3%. Table I lists the isotopic composition of the enriched cadmium used.

TABLE I. Isotopic composition of enriched[a] cadmium.

Mass number	Atom %
106	77.9
108	0.9
110	4.3
111	3.0
112	4.6
113	2.0
114	4.8
116	2.5

[a] The enriched isotope was obtained from the Isotopes Division, Oak Ridge National Laboratory.

B. Irradiations

The irradiations were performed in the external alpha-particle beam of the Brookhaven 60-in. cyclotron.

* Work supported by the U. S. Atomic Energy Commission.
† Present address: Analytical Chemistry Division, Oak Ridge National Laboratory, Oak Ridge, Tennessee.
[1] R. L. Hahn and J. M. Miller, Phys. Rev. 124, 1879 (1961).
[2] S. Fukushima, S. Hayashi, S. Kume, H. Okamura, K. Otozai, K. Sakamoto, and Y. Yoshizawa, Nucl. Phys. 41, 275 (1963).
[3] J. Blatt and V. F. Weisskopf, *Theoretical Nuclear Physics* (John Wiley & Sons, Inc., New York, 1952), Chaps. 6 and 8.
[4] I. Dostrovsky, Z. Fraenkel, and G. Friedlander, Phys. Rev. 116, 683 (1960).
[5] J. R. Huizenga and G. Igo, Nucl. Phys. 29, 462 (1962).

Several targets were bombarded concurrently by means of the stacked-foil method. Each target was placed in the stack so that the gold foil intercepted the alpha beam before the Cd^{106} deposit; aluminum foils, placed behind the cadmium, served both to catch recoil nuclei and to degrade the energy of the beam. The range-energy relations of Bichsel[6,7] for aluminum and gold were used to determine the energy of the alpha particles incident upon each cadmium target in the stack. Because the cadmium plates were all very thin ($\leqslant 0.600$ mg/cm^2), their effect on the energy of the alphas was neglected.

The energy of the incident beam was measured by determining the range of the alphas in aluminum and blue cellophane.[8] In this method, several pieces of blue cellophane, each equivalent in thickness to 4.5 mg/cm^2 of aluminum, are placed behind ≈ 150 mg/cm^2 of aluminum so that the thickness of the entire stack is greater than the range of 40-MeV alpha particles. Upon irradiation, the alphas traverse the aluminum and stop in the cellophane stack, thus bleaching some of the cellophane pieces. By measuring the relative bleaching of the cellophane pieces with an optical device, one can determine the range, and thus the energy, of the alpha beam. The number of alphas impinging on the target stack was measured in each irradiation by a calibrated charge integrator attached to the Faraday cup assembly.[9]

C. Chemical Separations

Anion exchange techniques[10] were utilized in order to separate the tin, indium, and cadmium cleanly and rapidly from one another. First the cadmium target was dissolved from the gold backing in a solution of 0.2N HCl which contained 1 mg each of indium and tin carriers; a drop or two of hydrogen peroxide accelerated the dissolution process. The aluminum recoil catcher was also dissolved in this solution. The solution was adjusted so that it was 0.1N in HCl and 1N in HF and then passed through a column of Dowex-1 resin which was pretreated with 0.1N HCl–1N HF.

Under these conditions, the indium, which adheres only slightly to the resin, could be removed while the tin and the cadmium remained on the column. Eluting with 0.001N HCl–1N HF then removed the cadmium; tin finally came off in a solution of 2N HCl–3N HF. The tin, indium, and cadmium samples were all precipitated as the sulfides and mounted for counting.

For the isolation of silver and palladium, usual techniques[11] involving precipitation of AgCl and palladium dimethyl glyoxime were employed.

D. Counting Techniques

All of the products formed in these irradiations are neutron-deficient; most of them have appreciable orbital electron-capture branches. In addition, for several of the products investigated, the decay schemes are not accurately known. Because of these considerations, 4π scintillation counting was initially chosen as the routine counting method in these experiments.

Two matched NaI(Tl) crystals, each 2 mm thick by 1.5 in. in diameter, were used as detectors; the arrangement of the crystals was such that the counting sample was placed in a reproducible manner between the two crystals. The effective solid angle subtended by a point source under these conditions was determined to be 98% of 4π. Only a lower level discriminator was used in the counter so that all radiations above some 10 or 15 keV gave rise to counts. It was found that positrons also were detected with high efficiency in the counter. This effect varied with the Z of the emitting nucleus. Thus for C^{11}, the detection efficiency was 0.78; for Mn^{51}, the value was 0.96; and for Mo^{91}, it was 1.0. Accordingly, the positron detection efficiency was taken to be unity. Taking into account the various probabilities for positron, x-ray, and gamma-ray detection, one can then calculate the over-all detection efficiency in the 4π counter as outlined in the Appendix. The decay scheme data used in the calculations were those currently appearing in the literature.[12] The efficiency values are listed in Table II. It should be noted that they are close to unity, so that alterations in the decay schemes should not drastically change these efficiencies.

Although the efficiencies for Sn^{110} and the indium isotopes are tabulated in Table II, difficulties in the decay-curve analyses, because of the presence of other isotopes of similar half lives, led to the use of differential gamma counting to determine the disintegration rates of Sn^{110}, In^{109}, In^{108}, and In^{107}. Also, to determine accurate ratios of the Sn^{109} to In^{109} and Sn^{108} to In^{108} cross sections, it was decided to count the tin isotopes via their indium daughters. Thus, the tin cross sections would be expressed in terms of the decay of the indium daughters, and the tin-to-indium ratios would be independent of uncertainties in counting efficiency or decay scheme.

The disintegration rate of a nuclide produced both by nuclear reaction and by radioactive decay of some other product of the irradiation can be written as

$$D_d(t_0) \propto \frac{\sigma_p}{(\lambda_d-\lambda_p)}\left[\lambda_d e^{-\lambda_p t}(1-e^{-\lambda_p T})-\lambda_p e^{-\lambda_d t}(1-e^{-\lambda_d T})\right] + \sigma_d e^{-\lambda_d t}(1-e^{-\lambda_d T}), \quad (1)$$

[6] H. Bichsel, R. F. Mozley, and W. A. Aron, Phys. Rev. **105**, 1788 (1957).
[7] H. Bichsel, Phys. Rev. **112**, 1089 (1958).
[8] J. B. Cumming (private communication).
[9] S. Amiel and N. T. Porile, Rev. Sci. Instr. **29**, 1112 (1958).
[10] F. Nelson, R. M. Rush, and K. A. Kraus, J. Am. Chem. Soc. **82**, 339 (1960).
[11] O. T. Høgdahl, *The Radiochemistry of Palladium* (National Academy of Sciences—National Research Council, Washington 25, D. C.), NAS-NS-**3052** (1961); D. N. Sunderman and C. W. Townley, *The Radiochemistry of Silver* (National Academy of Sciences—National Research Council, Washington 25, D. C.), NAS-NS-**3047** (1961).
[12] *Nuclear Data Sheets*, compiled by K. Way *et al.* (Printing and Publishing Office, National Academy of Sciences—National Research Council, Washington 25, D. C.).

TABLE II. Experimental parameters used in the determination of Cd^{106} excitation functions.

Isotope	Half-life	4π Efficiency[a]	Gamma-ray energy (MeV)[b]	Gamma-ray abundance[b]	Reference[c]
Sn^{110}	4.0 h	0.79	0.28	1.0	NRC-60-2-76
Sn^{109}	18 min	0.90	0.66		NRC-60-2-59
Sn^{108}	9.2 min		0.42, 0.28[d]		5-1-14
In^{109}	4.3 h	0.87	0.205	0.75	NRC-60-2-57, 58
In^{108}	40 min 58 min		0.63	1.0	5-1-13
In^{107}	33 min	0.91	0.22	0.46[e]	NRC-60-5-144
Cd^{109}	470 days	1.00			NRC-60-2-56
Cd^{107}	6.7 h	1.04			NRC-60-5-143
Cd^{105}	54.7 min	0.90			NRC-61-4-26
Ag^{105}	40 days	0.78			NRC-61-4-24, 25
Pd^{101}	8.5 h	0.81	0.29	0.15	NRC-61-2-35

[a] Detection efficiency of 4π scintillation counter.
[b] The gamma-ray energies and abundances are listed for those isotopes which were assayed by gamma-ray spectrometry.
[c] The NRC numbers refer to the page designations in *Nuclear Data Sheets* for the specific isotopes listed. See Ref. 12.
[d] These gammas were previously unreported.
[e] The abundance of the 0.22-MeV gamma ray in In^{107} was determined by use of 4π and differential gamma counting.

where subscripts p and d refer to parent and daughter, respectively, in the decay chain; $D_d(t_0)$ is the disintegration rate of the daughter nuclide at the time of chemical separation of parent and daughter; λ is the radioactive decay constant; T is the length of the irradiation; t is the interval between the end of bombardment and the chemical separation; and σ is the cross section for the nuclear reaction under consideration. As is seen from Eq. (1), rapid separation of indium from tin after a brief irradiation can be used to obtain a measure of σ_d, plus a contribution from σ_p. On the other hand, if the tin and indium are not separated until all of the tin has decayed ($e^{-\lambda_p t}=0$), a measure of the sum of σ_p and σ_d can be determined. (As an alternative method of obtaining the mass 109 yield, the tin and indium products were allowed to decay to Cd^{109}, which was then assayed in the 4π scintillation counter.) Then by combining the results from the rapid separations with the total tin-indium yield, one can determine the values of σ_p and σ_d.

Additional data on the shapes of the tin excitation functions were obtained in a few experiments by direct measurements of the tin yields by differential gamma spectrometry. Because the decay schemes of these isotopes are not well characterized, absolute cross sections could not be obtained from these measurements.

The various gamma rays which were observed in the cross section measurements are listed in Table II. It is of interest that two gamma rays, previously unreported, of 0.28 and 0.42 MeV, were found to be associated with the 9.2-min Sn^{108}. Also, it was found, by use of 4π and differential gamma counting, that the 0.22-MeV gamma ray of In^{107} occurs in only 0.46 of the decays.

An attempt was made, unsuccessfully, to measure the half-life of Sn^{107}, the $(\alpha,3n)$ product. From beta-decay systematics,[13] one would expect its decay energy to be greater than 4 MeV. If the transition is assumed to be normal allowed, with a logft value of about 5, a calculated half-life of about 2 min is obtained.[14] However, experiments in which distinctive gamma rays were sought very shortly after irradiation of Cd^{106} with 40-MeV alphas yielded no information on any new half-lives. Also, milking experiments in which indium was removed from tin at 2-min intervals proved inconclusive; no appreciable concentrations of In^{107} were found. Thus, it is concluded that the Sn^{107} half-life is probably much less than a minute; the data presented herein for In^{107} therefore represent the sum of the $(\alpha,3n)$ and $(\alpha,p2n)$ excitation functions.

III. RESULTS

Twenty-five irradiations were performed in the course of this work. A large majority of the cyclotron runs lasted less than ten minutes so that the short-lived nuclides produced from Cd^{106} could be isolated; several of the irradiations were of 3 to 4 h duration in order that measurable yields of long-lived products or of nuclides with low formation cross sections, as Sn^{110} and Pd^{101}, could be obtained. In those instances in which the irradiation times were comparable with the half-lives of the radioactive nuclei formed in the irradiations, variations in beam intensity during irradiation were taken into account in the cross-section calculations. Uncertainties in the experimental excitation functions are estimated to be about 8% for all of the reactions that were directly measured. These errors arise from counting statistics and decay-curve analyses, counting efficiency determinations, chemical-yield measurements, and uncertainties in the decay schemes. The Sn^{109} and Sn^{108} cross sections, obtained by effectively subtracting σ_d from the sum of σ_p and σ_d, consequently contain uncertainties of about 12% or greater. In addition, the results for In^{109} and In^{108} contain uncertainties resulting

[13] K. Way and M. Wood, Phys. Rev. 94, 119 (1954).

[14] G. Friedlander, J. W. Kennedy, and J. M. Miller, *Nuclear and Radiochemistry* (John Wiley & Sons, Inc., New York, 1964), pp. 245–250.

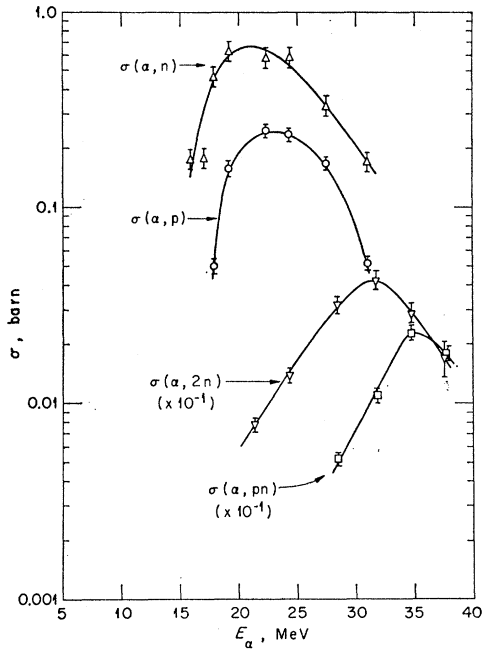

FIG. 1. Excitation functions for the reactions $Cd^{106}(\alpha,n)Sn^{109}$, $(\alpha,p)In^{109}$, $(\alpha,2n)Sn^{108}$, and $(\alpha,pn)In^{108}$. E_α is the energy of the α particle in the laboratory system.

from the rapid chemical separations of tin and indium. That is, although the separations were performed about 5 min after the irradiation, large corrections still had to be made for the number of daughter indium nuclei formed from tin during the irradiation and the 5-min interval. This effect is much more pronounced for mass 108 than mass 109 because of the shorter half-lives associated with the Sn^{108} and In^{108} products (see Table II).

The resulting excitation functions for mass 109 and 108 products are shown in Fig. 1. In the figure, one should note that the excitation functions for reactions involving proton emission have their maxima at energies about 3 MeV higher than those for the corresponding reactions involving neutrons only. Also, it is apparent that reactions involving the emission of protons can compete quite favorably with those in which only neutrons are emitted. The data presented for In^{109} resulted from observing the decay of the 4.3-h ground state; the yield of the 1.3-min isomeric state at 0.66 MeV was not observed. In all of the experiments involving In^{109}, sufficient time was allowed to elapse after the tin-indium separation so that the 1.3-min isomer, formed either by the (α,p) reaction or from the Sn^{109} parent, could decay to the ground state; the reported data therefore represent the total In^{109} yields.

The excitation functions obtained for the mass 108 products are worthy of comment in that they may be affected by some systematic errors. The decay schemes of neither Sn^{108} nor of the two In^{108} isomers are well known. Following the discussion above, it would be expected that, if the In^{108} isotope were used to determine all of the cross sections of mass 108 products, unknown quantities like branching ratios would not affect the ratio of Sn^{108} to In^{108}. However, an additional complication is the fact that In^{108} was assayed by measurement of the most abundant γ ray (0.63 MeV) which occurs in the decay of both isomeric states; moreover, the half-lives of the two isomers are very similar, namely, 40 and 58 min. Thus, the decay curves of the 0.63-MeV γ ray of In^{108} could not be resolved into separate contributions from the isomers. Instead, the decay curves were fitted with a value intermediate between the actual half-lives of the two states; this "average" value varied from 47 to 49 min. The "average" tin and indium cross sections were then computed from Eq. (1), using the average value of the half-life found for In^{108}. If this approximation using an intermediate half-life for In^{108} is a valid one, the difference in yields of the two In^{108} isomeric states, due both to the decay of Sn^{108} and to the variation of indium isomer production with energy, will be properly reflected in the values found for σ_p and for σ_d. However, the average half-life value used is about 20% different from the half-life of either isomer, so that the use of an intermediate half-life does introduce additional uncertainties into the cross section values found for the 108 chain. It should be noted, though, that the fact that all of the In^{108} data could be fitted with an essentially constant half-life indicates that the relative yields of the In^{108} isomers did not change drastically in the various experiments performed.

The excitation function for In^{107}, which represents the

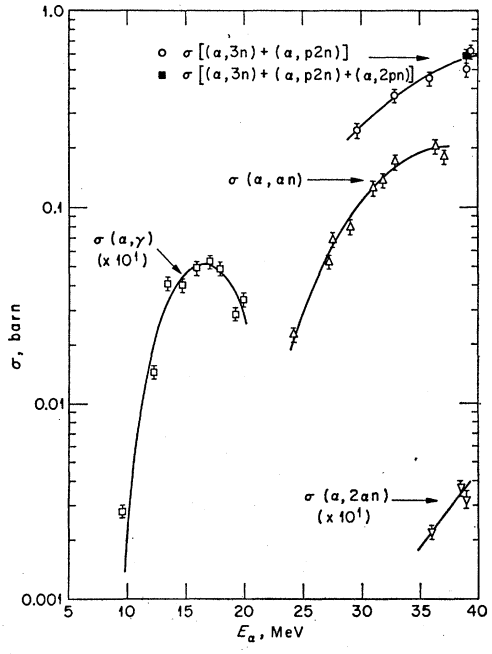

FIG. 2. Excitation functions for the reactions $Cd^{106}(\alpha,\gamma)Sn^{110}$, $(\alpha,3n)Sn^{107}+(\alpha,p2n)In^{107}$, $(\alpha,\alpha n)Cd^{105}$, and $(\alpha,2\alpha n)Pd^{101}$. E_α is the α-particle energy in the laboratory system.

TABLE III. Experimental cross sections (millibarns).

α-particle energy (MeV)	(α,γ)	(α,n)	(α,p)	$(\alpha,2n)$	(α,pn)	$[(\alpha,3n)+(\alpha,p2n)]$	$(\alpha,\alpha n)$	$(\alpha,2\alpha n)$
6.3	0.043							
9.5	0.28							
12.2	1.45							
13.3	4.12							
14.6	4.02							
15.8	4.92	174						
17.0	5.30	177						
17.9	4.90	461	50.0					
19.2	2.86	626	157					
19.9	3.37							
21.4				77.5				
22.3		574	243					
24.3		581	230	138			22.6	
27.2							53.0	
27.5		330	167				68.6	
28.5				318	52.0			
29.0							79.5	
29.6						246		
31.0		170	52.0				126	
31.8				427	110		138	
32.9						369	170	
34.8				287	230			
35.8						449		
36.0								0.22
36.3							205	
37.2							181	
37.7				169	180			
38.4								0.37
39.0						503		0.32
39.3						618		

sum of the cross sections for the $(\alpha,3n)$ and $(\alpha,p2n)$ reactions, is shown in Fig. 2. Because of the high threshold for the reaction, the experimental curve does not exhibit a peak in the energy interval investigated. Experiments were also performed in which the Sn^{107} and In^{107} were allowed to decay completely to Cd^{107} so that the sum of the $(\alpha,3n)$, $(\alpha,p2n)$, and $(\alpha,2pn)$ reactions was measured. As indicated in Fig. 2 by the point at 39 MeV, this sum does not deviate from the In^{107} curve; therefore, one may conclude that the cross section for the $(\alpha,2pn)$ reaction is small compared to the measured In^{107} cross section.

The data for the reactions leading to Cd^{105} and Pd^{101}, namely, the $(\alpha,\alpha n)$ and $(\alpha,2\alpha n)$ excitation functions, are also presented in Fig. 2. The $(\alpha,\alpha n)$ reaction does not reach a maximum below $\approx$40 MeV; its value at 37 MeV is 205 mb. The $(\alpha,2\alpha n)$ reaction has a high threshold and a low cross section; its value at 38 MeV is 0.37 mb. Measurements in which the sum of Cd^{105} and Ag^{105} was obtained also indicate that the ratio of $(\alpha,\alpha p)$ to $(\alpha,\alpha n)$ cross sections is very small.

The (α,γ) excitation function, which too is presented in Fig. 2, has quite a sharp maximum, with a peak cross section of 5.3 mb at 17 MeV and a full width at half maximum of about 6 MeV. The 1% of Cd^{108} in the target material can contribute to the production of Sn^{110} via the $(\alpha,2n)$ reaction. But the threshold for this reaction is 18.6 MeV, so that the observed Sn^{110} excitation function is considered to be, over most of the energy interval examined, a measure of the (α,γ) reaction on Cd^{106}.

The experimentally determined cross sections, which appear in Figs. 1 and 2, are listed in Table III.

IV. DISCUSSION

The sum of the experimentally determined excitation functions, or rather the sum of cross-section values taken at given energy intervals from the smoothed excitation function curves, is compared in Fig. 3 with calculated estimates of $\sigma_{R\alpha}$, the total reaction cross section for α particles. The optical model curve is based on the calculations of Huizenga and Igo[5] and is interpolated from their values for $_{41}Nb^{93}$, $_{45}Rb^{103}$, and $_{50}Sn^{119}$. For the continuum theory computation, the approximation given by Dostrovsky *et al.*[4] for the variation of the cross section with ϵ_α, the energy of the α particle, was used:

$$\sigma_{R\alpha}=\sigma_g(1+c_\alpha)(1-k_\alpha V_\alpha/\epsilon_\alpha). \quad (2)$$

The value of the nuclear radius parameter, which enters in the evaluation of both the geometric cross section σ_g and the Coulomb barrier V_α was taken to be $r_o=1.7$ F; this choice of r_o also determined the constants c_α and k_α.[4]

The experimental data presented in Fig. 3 include the results for all of the major reactions of Cd^{106} with α particles; only the yields of the $(\alpha,2p)$ and $(\alpha,\alpha\gamma)$ reactions, which could not be measured, are not included. The data, above 27 MeV, agree rather well with

the continuum theory results, while at lower energies, the calculation seems to underestimate the value of $\sigma_{R\alpha}$. It may be that the approximate form used for $\sigma_{R\alpha}$, especially in the vicinity of threshold, is responsible for this effect. Contrastingly, the optical-model prediction of $\sigma_{R\alpha}$ appears to be too high over most of the energy range investigated, It should again be noted that the largest contributors to the total cross-section curve, namely the mass 109, 108, and 107 products, were all measured via the respective indium isotopes. Thus, possible uncertainties in the various decay scheme parameters may have introduced some systematic errors into the cross-section values. For example, the dip observed in the data at about 24 MeV may possibly be due to a systematic overestimation of the mass 109 cross sections.

Comparison of the excitation functions in Figs. 1 and 2 with similar reaction curves[1] for Sn^{124} clearly demonstrates that the emission of charged particles is more probable for neutron-deficient Cd^{106} than for neutron-excess Sn^{124}. For example, the maximum cross sections (mb) measured for the (α,p), (α,pn), and $(\alpha,\alpha n)$ reactions, respectively, are Cd^{106}: 243, 230, and 205; Sn^{124}: 19, 49, and 60. This tendency favoring charged particle production in the neutron-deficient target may be graphically demonstrated by plotting the variation of σ_C/σ_N with excitation energy. (In converting to excitation energy, the separation energy of the α particle in Sn^{110} was taken to be 0.24 MeV.) Here, σ_C is the sum of cross sections at a given energy for those reactions in which *at least* one charged particle is emitted, regardless

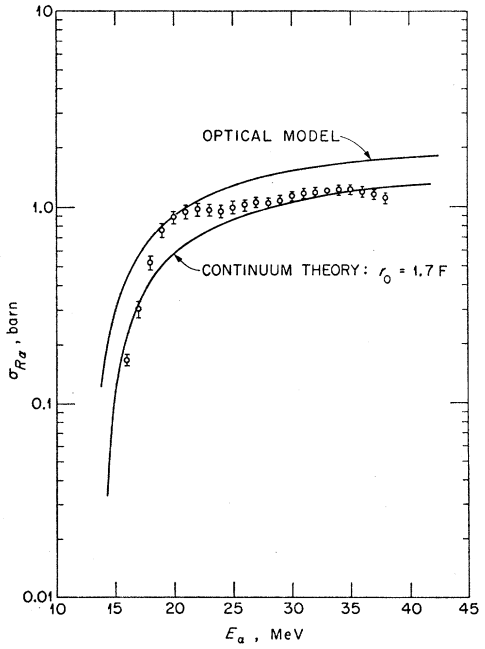

FIG. 3. The experimental total cross-section curve for Cd^{106} compared with the results of the optical model (see Ref. 5) and continuum theory (see Ref. 4). E_α is the α-particle energy in the laboratory system.

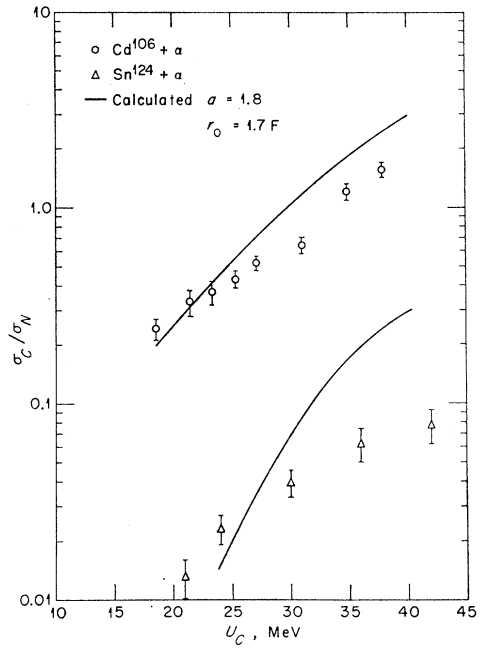

FIG. 4. Comparison of experimental and calculated values for Cd^{106} and Sn^{124} of σ_C/σ_N, the ratio of the sums of reactions involving, respectively, charged particles and neutrons, See text. U_C is the excitation energy of compound nucleus Sn^{110}.

of whether any neutrons are also emitted. The sum of cross sections for which *only* neutrons are emitted is given by σ_N. In Fig. 4, σ_C/σ_N, obtained from the various smoothed excitation functions, is plotted for Cd^{106} and Sn^{124}. The cadmium points above 29 MeV include values for the $(\alpha,3n)$ and $(\alpha,p2n)$ reactions; since these cross sections were not separately measured in this work, they were simply assumed to be equal so that the ratio σ_C/σ_N could be evaluated. Also, the contribution of the unmeasured $(\alpha,2n)$ reaction of Sn^{124} was approximated with the aid of the calculated total reaction cross-section curve.[1] But, despite the uncertainties in the ratios, it is clear that σ_C/σ_N is at least an order of magnitude larger for Cd^{106} than for Sn^{124}. Examination of the separation energies[12] of neutrons and protons in the various nuclei produced from Cd^{106} and Sn^{124} offers a partial explanation of this effect. For most of the nuclides arising from Cd^{106}, the separation energy of the last proton is $\sim$2–5 MeV less than that of the least bound neutron. This reduction in separation energy partially cancels the effect of the Coulomb barrier and allows the emission of charged particles to compete effectively with that for neutrons. For the products formed from Sn^{124}, the neutron separation energy is approximately equal to, or a few MeV less than, the proton separation energy. Charged particle emission is accordingly much less prevalent than neutron emission.

This apparent importance of separation energies in nuclear reactions is perhaps indicative of the decay of a compound nucleus. That is, the relative rates, Γ_n/Γ_p,

of neutron and proton evaporation from a compound nucleus may be expressed in the constant-temperature model as

$$\Gamma_n/\Gamma_p \propto \exp[(S_n-S_p-V_p)/T], \quad (3)$$

where S is the particle's separation energy; V, the Coulomb barrier; and T, the nuclear temperature.[15] Conversely, one may consider that in a direct interaction process involving the incident particle and a few nucleons of the target nucleus, with accompanying large transfer of momentum and kinetic energy, the resulting reaction rate should not be a very sensitive function of the binding-energy differences.

Unfortunately, detailed expressions for the evaluation of direct interaction rates are not available for straightforward comparison with excitation function data, although the calculations of Brown and Muirhead[16] have been used in studies of neutron-induced reactions.[17,18] Thus, one must rely mainly upon the statistical theory of nuclear reactions[19,20] for a quantitative discussion of the experimental results. In this model, the formation and decay of the excited compound nucleus are assumed to be independent processes. An important quantity in the calculation of the probabilities of the various decay modes is the level density $\rho(u)$ of the residual nucleus at energy u. Often, $\rho(u)$ is taken to be the level density of a Fermi degenerate gas[21]

$$\rho(u)=C\exp(2a^{1/2}u^{1/2}), \quad (4)$$

with C and a serving as parameters; a should, however, be proportional to the mass number, A. In Eq. (4), $u=(U-S_i-\delta)$, where U is the excitation energy of the compound nucleus, S_i is the separation energy of particle i, and δ is a measure of the pairing energy.[4]

The calculations of the relative reaction probabilities by the statistical theory were performed on the IBM-7090. Two modifications, by Porile[22] and Dresner,[23] of the original Monte Carlo program of Dostrovsky *et al.*[4] were used. Values of δ taken from Cameron,[24] and of nuclear masses tabulated by Wapstra[25] and Huizenga,[26] were used in the computations; for nuclei for which no mass measurements were available, mass values were calculated with Cameron's[27] semiempirical binding-energy formula.

As in the case of Sn^{124}, it was found that small values of the level density parameter, $a\approx 2$/MeV, were required to fit the Cd^{106} data. Larger values of $a\propto A$, which are expected for a Fermi gas, lead to low values of those cross sections that involve charged particle emission. These results agree with the findings of other workers, such as Swenson and Cindro,[28] who determined a in their studies of (α,p) reactions to be 3.2 and 3.9, respectively, for Pd^{106} and Sn^{118}. Also, Fukushima *et al.*[2] found $a=3$ from their investigation of the reactions of α particles with Ag^{107}. Grover[29] has explained these low a values as being due to the neglect of competitive gamma-ray de-excitation of the compound nucleus. Thus, he found $a\approx 2.8$ for the reaction $Sm^{144}(\alpha,3n)Gd^{145}$ when the usual evaporation calculation, ignoring gamma-ray emission, was performed; taking this additional mode of de-excitation into account gave a value of $a\sim 0.1A$.

To carry out the evaporation calculation, as outlined by Grover, requires detailed knowledge of the level schemes of the various nuclei involved in the reaction. This information is lacking for the nuclides produced in the present work, so that gamma-ray emission was ignored, and the value $a=A/60=1.8$ used in the calculations.

As seen in Fig. 4, although the results of the calculation do not agree in detail with the data, they certainly reproduce the trend that σ_C/σ_N is much larger for Cd^{106} than for Sn^{124}. The statistical theory calculation thus depends sensitively upon the various particle separation energies.

A more detailed comparison of the evaporation calculation with the data is given in Fig. 5, where cross-section ratios are plotted versus excitation energy. The agreement between theory and experiment for the reactions in which only one particle is emitted is quite good. However, the agreement is rather poor for the ratio $\sigma(\alpha,pn)/\sigma(\alpha,2n)$. Plotting the calculated cross sections in Fig. 6, rather than their ratios, shows that although both the $(\alpha,2n)$ and (α,pn) calculated curves do not follow the data very well, the greatest discrepancy exists for the (α,pn) results. It may be that uncertainties in separation energies account for this effect. Also, as discussed above, the data involving In^{108} may contain some systematic errors. In the case of the (α,n) and (α,p) curves, the observed differences between calculation and experimental results, as shown in Fig. 6, may be attributed to the use of the continuum theory formation cross sections in the calculation, since the calculated ratio of these excitation functions fits the data very well. As had been found with the Sn^{124} results, the (α,n) and (α,p) theoretical curves decrease more rapidly at higher energies than do the data, indicating some contribution of noncompound processes to these reactions beyond $\sim$27 MeV. However, these high-energy tails are not as pronounced as are those observed

[15] D. Bodansky, Ann. Rev. Nucl. Sci. **12**, 79 (1962).
[16] G. Brown and H. Muirhead, Phil. Mag. **2**, 473 (1957).
[17] R. F. Coleman, B. E. Hawker, L. P. O'Connor, and J. L. Perkin, Proc. Phys. Soc. (London) **73**, 215 (1959).
[18] J. F. Barry, R. F. Coleman, B. E. Hawker, and J. L. Perkin, Proc. Phys. Soc. (London) **74**, 632 (1959).
[19] N. Bohr, Nature **137**, 344 (1936).
[20] V. F. Weisskopf, Phys. Rev. **52**, 295 (1937).
[21] T. Ericson, Phil. Mag. Suppl. **9**, 425 (1960).
[22] N. T. Porile (private communication).
[23] L. Dresner (private communication).
[24] A. G. W. Cameron, Can. J. Phys. **36**, 1040 (1958).
[25] A. M. Wapstra, Physica **21**, 367 (1955).
[26] J. R. Huizenga, Physica **21**, 410 (1955).
[27] A. G. W. Cameron, Can. J. Phys. **35**, 1021 (1957).
[28] W. Swenson and N. Cindro, Phys. Rev. **123**, 910 (1961).
[29] J. R. Grover, Phys. Rev. **123**, 267 (1961).

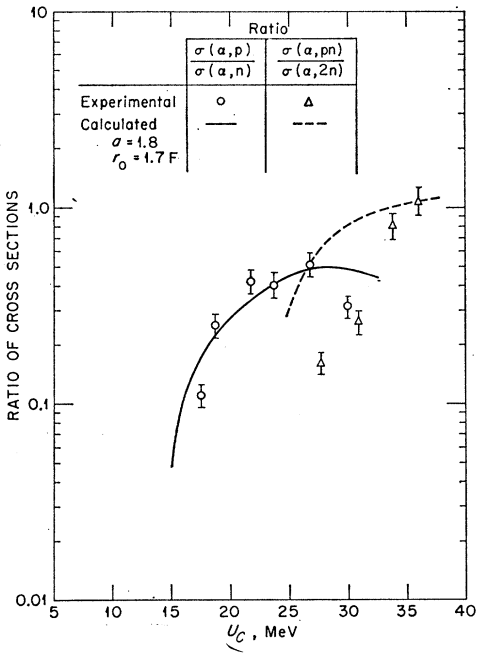

FIG. 5. Comparison of experimental and calculated ratios for Cd^{106} of $\sigma(\alpha,p)/\sigma(\alpha,n)$ and $\sigma(\alpha,pn)/\sigma(\alpha,2n)$. U_C is the excitation energy of compound nucleus Sn^{110}.

in the (α,n) and (α,p) reactions on Sn^{124}. It would appear, then, as one proceeds from a neutron-excess nucleus like Sn^{124} to a neutron-deficient one like Cd^{106}, that the increased probability for charged-particle emission that is encountered, which is equivalent to an increase in the various evaporation channels available to an excited nucleus, thus leads to a decrease in the probability that a nonstatistical process will occur.

The $(\alpha,\alpha n)$ reaction on Cd^{106} also seems to be predominantly a compound-nuclear process, as does this reaction[30] on Sn^{124}. These reactions and the results of the statistical theory are shown in Fig. 7. The shape and magnitude of the calculated excitation functions are in good agreement with the data.

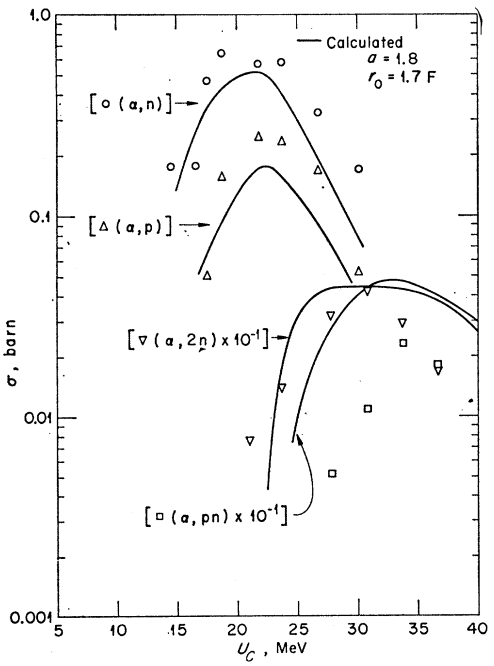

FIG. 6. Comparison of experimental and theoretical values of the cross sections for the reactions $Cd^{106}(\alpha,n)$, (α,p), $(\alpha,2n)$, and (α,pn). U_C is the excitation energy of compound nucleus Sn^{110}.

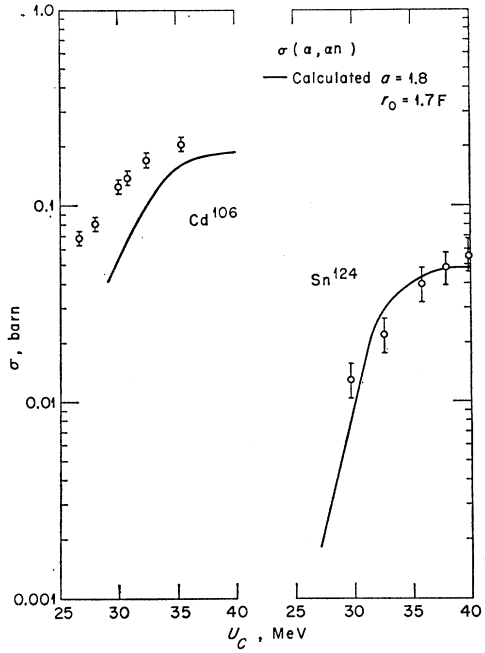

FIG. 7. Comparison of experimental and calculated excitation functions for $(\alpha,\alpha n)$ reactions on Cd^{106} and Sn^{124}. U_C is the excitation energy of the respective compound nuclei, Sn^{110} and Te^{128}.

ACKNOWLEDGMENTS

I wish to thank Dr. G. Friedlander for encouragement in this work and for several illuminating discussions. The cooperation of Dr. C. P. Baker and the operating crew of the BNL 60-in. cyclotron was essential to the completion of this work. Many thanks are expressed to the members of the Analytical Chemistry Group, to Dr. R. W. Stoenner, and especially to Dr. K. Rowley, for performing the chemical yield determinations.

V. APPENDIX: PROBABILITY OF DETECTING AN EVENT IN THE 4π SCINTILLATION COUNTER

Consider a nuclide which decays mainly by orbital-electron capture, plus some positron emission, followed

[30] The calculation previously performed for the $Sn^{124}(\alpha,\alpha n)$ reaction was not as accurate as that carried out by the Monte Carlo method. See Ref. 1.

by a cascade of n gamma rays to the ground state. The probability of detection[31] then is

$$P=1-(1-P_e-P_\beta)[\prod_n(1-P_{\gamma n}-P_{Cn})], \quad \text{(A1)}$$

where P_e is the probability of detecting electron capture, P_β is the probability of detecting a positron, $P_{\gamma n}$ is the probability of detecting the nth gamma, and P_{Cn} is the probability of detecting internal conversion of the nth gamma.

In this experiment, only capture or conversion processes resulting in the emission of K x rays are detected. X rays from the L and higher shells, Auger electrons, and weak conversion electrons are not counted. Thus

$$P_e=e[K/(K+L+M)]\omega_K g f_K i_K, \quad \text{(A2)}$$

where e is the probability that the decay occurs by electron capture; $K/(K+L+M)$ is the fraction of captures that occur in the K shell; and ω_K (the fluorescence yield) is the number of K x rays emitted per K vacancy. g is the geometry factor; i, the intrinsic efficiency of the NaI(Tl) crystal ($i_K=1$); and f, the self-absorption factor. The factor i was calculated for a finite crystal following the method of Axel[32] using total absorption coefficients of NaI.

Similarly,

$$P_\beta=bgf_\beta i_\beta. \quad \text{(A3)}$$

$i_\beta=1$, and $f_\beta=1$, were used in all cases since the positron energies were greater than 1 MeV. b is the probability that the decay occurs through positron emission. The values of e and b, assuming that the transitions are allowed, were determined from beta-decay theory,[33] with the condition that $e+b=1$. Whenever possible, experimental values of e and b[12] were used to check the calculations.

For the gamma cascade,

$$P_{\gamma n}=gf_\gamma i_\gamma/(1+\alpha_T), \quad \text{(A4)}$$

$$P_{Cn}=\omega_K g f_K i_K \alpha_K/(1+\alpha_T), \quad \text{(A5)}$$

where α_K is the internal conversion coefficient for the K shell, and α_T is the total conversion coefficient. Values of $K/(K+L+M)$,[34] α_K and α_T[35] were obtained from theoretical compilations, or if possible, from decay scheme data.[12] The multipolarities of the various gamma-ray transitions were taken from the literature.[12] When these were not known, $E2$ transitions were assumed.

More complicated decays, involving several decay branches and states with finite lifetimes, can be treated by a simple generalization of Eq. (A1). For example, in the decay[12] of Cd^{109}, the electron capture leads to a state at 0.088 MeV that decays with a half-life of 40 sec. Since this delay is long compared to the resolving time of the counter, the events due to the electron capture and to the 0.088-MeV state are additive. That is, the probability of detection of Cd^{109} is, with $P_\beta=0$,

$$P=1-(1-P_e)+1-(1-P_\gamma-P_C)=P_e+P_\gamma+P_C.$$

Using Eqs. (A2), (A4), and (A5), one obtains $P_e=0.626$, $P_\gamma=0.038$, and $P_C=0.338$; the total detection probability is then 1.00.

---

[31] M. Deutsch and O. Kofoed-Hansen, in *Experimental Nuclear Physics*, edited by E. Segrè (John Wiley & Sons, Inc., New York, 1959), Vol. III, pp. 432–437.

[32] P. Axel, Rev. Sci. Instr. **25**, 391 (1954); P. Axel, Brookhaven National Laboratory Report BNL-271, 1953 (unpublished).

[33] M. L. Perlman and M. Wolfsberg, Brookhaven National Laboratory Report BNL-485, 1958 (unpublished).

[34] H. Brysk and M. E. Rose, Oak Ridge National Laboratory Report ORNL-1830, 1955 (unpublished); H. Brysk and M. E. Rose, Rev. Mod. Phys. **30**, 1169 (1958).

[35] M. E. Rose, *Internal Conversion Coefficients* (North-Holland Publishing Company, Amsterdam, 1958).